J|A|C|S
ARTICLES
Published on Web 05/01/2002

Mechanism of Acetylcholinesterase Inhibition by Fasciculin: A 5-ns Molecular Dynamics Simulation

Kaihsu Tai,*,† Tongye Shen,‡ Richard H. Henchman,† Yves Bourne,§ Pascale Marchot,|| and J. Andrew McCammon*,†,⊥

Contribution from Howard Hughes Medical Institute and Departments of Chemistry and Biochemistry, of Pharmacology, and of Physics, University of California, San Diego, La Jolla, California 92093-0365; Architecture et Fonction des Macromolécules Biologiques, CNRS UMR-6098, Institut de Biologie Structurale et Microbiologie, Marseille, France; and Ingenierie des Protéines, CNRS UMR-6560, Institut Fédératif de Recherche Jean Roche, Université de la Méditerranée, Marseille, France

Received October 16, 2001

Abstract: Our previous molecular dynamics simulation (10 ns) of mouse acetylcholinesterase (EC 3.1.1.7) revealed complex fluctuation of the enzyme active site gorge. Now we report a 5-ns simulation of acetylcholinesterase complexed with fasciculin 2. Fasciculin 2 binds to the gorge entrance of acetylcholinesterase with excellent complementarity and many polar and hydrophobic interactions. In this simulation of the protein−protein complex, where fasciculin 2 appears to sterically block access of ligands to the gorge, again we observe a two-peaked probability distribution of the gorge width. When fasciculin is present, the gorge width distribution is altered such that the gorge is more likely to be narrow. Moreover, there are large increases in the opening of alternative passages, namely, the side door (near Thr 75) and the back door (near Tyr 449). Finally, the catalytic triad arrangement in the acetylcholinesterase active site is disrupted with fasciculin bound. These data support that, in addition to the steric obstruction seen in the crystal structure, fasciculin may inhibit acetylcholinesterase by combined allosteric and dynamical means. Additional data from these simulations can be found at http://mccammon.ucsd.edu/.

Introduction

Acetylcholinesterase (AChE; EC 3.1.1.7) terminates synaptic transmission at cholinergic synapses by catalyzing hydrolysis of the neurotransmitter acetylcholine.[1] A gorge, 2 nm in depth, leads from the surface of the enzyme to its buried active site. Fasciculin 2 (Fas2), a peptidic three-finger snake toxin (61 residues) from green mamba (*Dendroaspis angusticeps*) venom, is a picomolar inhibitor of mammalian acetylcholinesterases.

Much kinetics and structural information for the fasciculin 2−mouse acetylcholinesterase complex (Fas2−mAChE) has been collected in the past decade. Some kinetic data suggested that the inhibition may be achieved by steric obstruction: Fas2 capping the entrance of the gorge, sterically blocking the entry of the ligand.[2] The crystallographic structures of complexes of Fas2 with mouse acetylcholinesterase,[3] *Torpedo californica* AChE,[4] and human AChE[5] all supported this hypothesis and showed excellent surface complementarity between Fas2 and AChE. The contacts between Fas2 and mAChE are in turn verified by mutation studies.[6−8]

In the crystal structures, allosteric effects seem to be subtle at most. However, this has not been fully reconciled with kinetics information, which shows residual catalytic activity for the Fas2-bound enzyme. Indeed, inhibition of AChE by fasciculin, despite its high affinity and slow rate of dissociation, is not complete, and the fractional residual activity reveals that substrates can still enter the active site in Fas2-bound AChE.[6,9−12] With certain AChE mutants and substrates whose catalysis is not diffusion-limited, Fas2 even acts as an allosteric activator,[13] connoting possible influence by Fas2 on alternative passages

† Department of Chemistry and Biochemistry, University of California, San Diego.
‡ Department of Physics, University of California, San Diego.
§ Institut de Biologie Structurale et Microbiologie.
|| Université de la Méditerranée.
⊥ Howard Hughes Medical Institute and Department of Pharmacology, University of California, San Diego.

(1) Kandel, E. R.; Schwartz, J. H.; Jessell, T. M. *Principles of Neural Science*, 3rd ed.; Appleton & Lange: Norwalk, CT, 1991.
(2) Rosenberry, T. L.; Rabl, C.-R.; Neumann, E. *Biochemistry* **1996**, *35*, 685−690.
(3) Bourne, Y.; Taylor, P.; Marchot, P. *Cell* **1995**, *83*, 503−512.
(4) Harel, M.; Kleywegt, G. J.; Ravelli, R. B. G.; Silman, I.; Sussman, J. L. *Structure* **1995**, *3*, 1355−1366.
(5) Kryger, G.; Harel, M.; Giles, K.; Toker, L.; Velan, B.; Lazar, A.; Kronman, C.; Barak, D.; Ariel, N.; Shafferman, A.; Silman, I.; Sussman, J. L. *Acta Crystallogr.* **2000**, *D56*, 1385−1394.
(6) Radić, Z.; Duran, R.; Vellom, D. C.; Li, Y.; Cerveñansky, C.; Taylor, P. *J. Biol. Chem.* **1994**, *269*, 11233−11239.
(7) Marchot, P.; Prowse, C. N.; Kanter, J.; Camp, S.; Ackermann, E. J.; Radić, Z.; Bougis, P. E.; Taylor, P. *J. Biol. Chem.* **1997**, *272*, 3502−3510.
(8) Marchot, P.; Bourne, Y.; Prowse, C. N.; Bougis, P. E.; Taylor, P. *Toxicon* **1998**, *36*, 1613−1622.
(9) Marchot, P.; Khélif, A.; Ji, Y. H.; Mansuelle, P.; Bougis, P. E. *J. Biol. Chem.* **1993**, *268*, 12458−12467.
(10) Eastman, J.; Wilson, E. J.; Cerveñansky, C.; Rosenberry, T. L. *J. Biol. Chem.* **1995**, *270*, 19694−19701.
(11) Šentjurc, M.; Pečar, S.; Stojan, J.; Marchot, P.; Radić, Z.; Grubič, Z. *Biochim. Biophys. Acta* **1999**, *1430*, 349−358.
(12) Radić, Z.; Taylor, P. *J. Biol. Chem.* **2001**, *276*, 4622−4633.
(13) Radić, Z.; Quinn, D. M.; Vellom, D. C.; Camp, S.; Taylor, P. *J. Biol. Chem.* **1995**, *270*, 20391−20399.

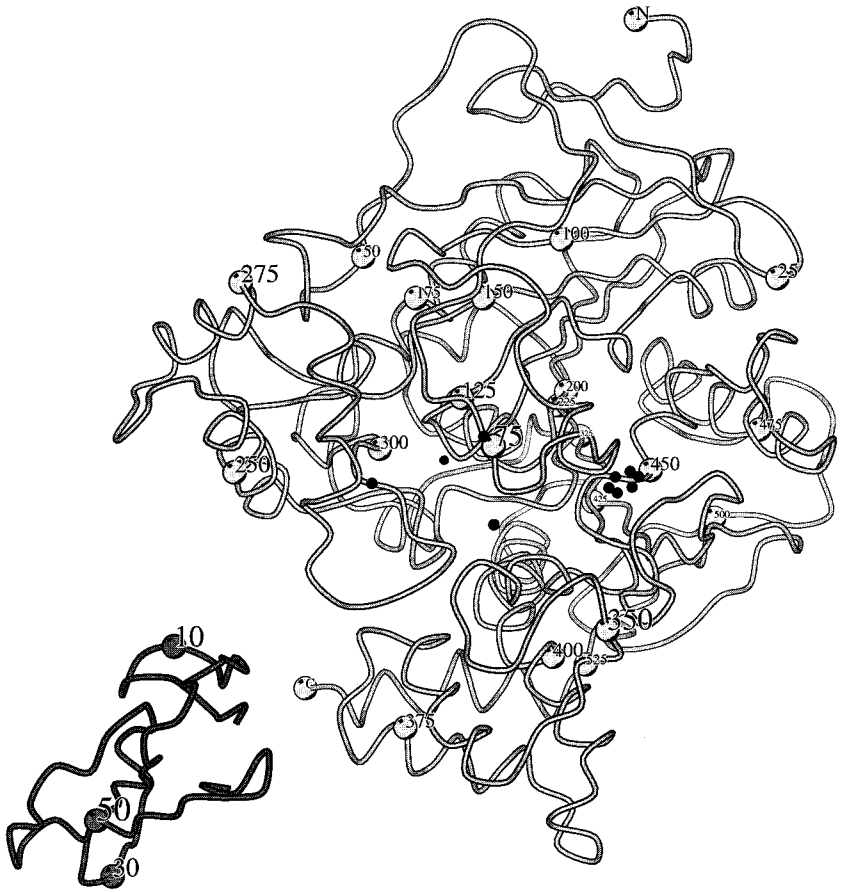

Figure 1. Overview of the Fas2−mAChE complex structure (1KU6). The mAChE molecule is labeled every 25 residues; the Fas2 molecule, moved from the mAChE for the sake of clarity, has residues 10 (in loop I), 30 (in loop II) and 50 (in loop III) labeled. The mAChE atoms that are used to define the blocking sphere (see Methods) for each passage are marked with small spheres: gorge (Tyr 72 OH, Leu 76 $C_{\delta 1}$, Trp 286 C_{β}); side door (Thr 75 C_{β}); back door (Tyr 449 six-membered ring). Generated using Molscript.[43]

and other interaction in addition to direct steric occlusion. Moreover, it has been suggested that Fas2 alters the conformation of AChE in the active site[10] and in the Ω loop (Cys 69−Cys 96),[3,14−16] particularly that of the Trp 86 side chain.[13]

We previously carried out a 10-ns molecular dynamics (MD) simulation of mAChE.[17] This has revealed the complex nature of the gorge fluctuations. Collective motions on many scales contribute to the opening behavior of the gorge, and two distinct states, one narrow and one wide, were found. Correlation results identified the motions of many protein residues as the gorge opens. In particular, the residues within the mAChE moiety that includes the gorge apparently move away from the gorge entrance when the gorge opens. The opening of alternative passages to the active site was found to be infrequent, since less than one-hundredth of the frames collected showed opening of alternative passages. These alternative passages are the back door, bounded by residues Trp 86, Tyr 449, and Ile 451,[18] and the side door, bounded by residues Thr 75, Leu 76, and Thr 83.[19,20]

To investigate the structural and dynamical effect of Fas2 binding on mAChE, we performed another MD simulation of the mAChE complexed with Fas2 and compared mAChE properties with the results from the previous apo-mAChE trajectory.

Methods

Crystal Structure. The crystal structure of the Fas2−mAChE complex used for this study (Protein Data Bank identification code, 1KU6) was refined to 0.25-nm (2.5-Å) resolution. It contains one Fas2 molecule (residues 1−61) bound to one mAChE monomer (residues 3−541), one GlcNAc moiety linked to mAChE residue Asn 350, one ethylene glycol, and 189 water molecules. The overall deviations from ideal geometry are 0.010 Å for bond distances and 1.76° for bond angles. This structure, though virtually identical to the previous complex structure 1MAH[3] with an average root-mean-square deviation (RMSD) of 0.57 Å for 587 C_{α} atoms, provides significantly improved accuracy in the positions of the main and side chains of Fas2 and mAChE and of those located at the complex interface and unambiguously reveals the position of a higher number of water molecules. A detailed description of this structure including a report on the crystallization and data collection conditions will be published elsewhere.

Molecular Dynamics Simulation. The 0.25-nm crystal structure of Fas2−mAChE described above was used to build the initial structure (Figure 1; Supporting Information). In addition to the Fas2 and mAChE

(14) Szegletes, T.; Mallender, W. D.; Thomas, P. J.; Rosenberry, T. L. *Biochemistry* **1999**, *38*, 122−133.
(15) Mallender, W. D.; Szegletes, T.; Rosenberry, T. L. *Biochemistry* **2000**, *39*, 7753−7763.
(16) Shi, J.; Boyd, A. E.; Radić, Z.; Taylor, P. *J. Biol. Chem.* **2001**, *276*, 42196−42204.
(17) Tai, K.; Shen, T.; Börjesson, U.; Philippopoulos, M.; McCammon, J. A. *Biophys. J.* **2001**, *81*, 715−724.
(18) Gilson, M. K.; Straatsma, T. P.; McCammon, J. A.; Ripoll, D. R.; Faerman, C. H.; Axelsen, P. H.; Silman, I.; Sussman, J. L. *Science* **1994**, *263*, 1276−1278.
(19) Wlodek, S. T.; Clark, T. W.; Scott, L. R.; McCammon, J. A. *J. Am. Chem. Soc.* **1997**, *119*, 9513−9522.
(20) Tara, S.; Straatsma, T. P.; McCammon, J. A. *Biopolymers* **1999**, *50*, 35−43.

molecules themselves, the 189 crystallographic water molecules present in the structure were left intact and considered part of the solvent throughout the following preparation.

To mend the missing or truncated residues and segments of the Fas2−mAChE crystal structure 1KU6, we used mAChE segment Pro 258−Gly 264 from the mAChE crystal structure (1MAA);[21] mAChE residues Lys 496, Ala 542, and Thr 543 from the previous Fas2−mAChE crystal structure (1MAH); and Fas2 residue Lys 51 from the unliganded Fas2 crystal structure (1FSC).[22] The mAChE residue Arg 493, which in the structure was modeled as an alanine residue due to side-chain mobility, was kept unchanged, following our previous simulation of mAChE.[17,20] In the end, the prepared structure has the same mAChE atoms as our previous apo-mAChE MD. These structure manipulations were carried out using Insight II (Accelrys, San Diego, CA).

The following preparation, minimization, and MD procedures were performed using NWChem version 4.0,[23] AMBER 95 force field[24] for the solutes (proteins and counterions), and SPC/E[25] for the water molecules.

Hydrogen was added to the structure using the prepare module of NWChem. To neutralize the −6 charge of the Fas2−mAChE complex, six sodium counterions were added; in addition to the sodium ion in the active site as in the previous simulation of apo-mAChE,[17,20,] the position of the other five counterions are analogous to those farthest from Fas2 in the previous mAChE simulation. The longest dimension of the molecule is 8.4 nm at this point. The molecule is then solvated in a cubic box of water molecules with length 10.5 nm on each side.

The MD simulation was performed in the isothermal−isobaric ensemble. The solvent and solute were separately coupled to temperature reservoirs of 298.15 K with coupling times of 0.1 ps; pressure was restrained to 1.025×10^5 Pa with a coupling time of 0.5 ps.[26] The MD simulation time step was 2 fs for both equilibration and production. Long-range electrostatic interactions were calculated using particle-mesh Ewald summation.[27] Bond lengths between hydrogens and heavy atoms were constrained using SHAKE.[28,29]

The water molecules were relaxed using steepest descent for 5000 steps and equilibrated at 298.15 K for 100 ps. The whole MD simulation system contained 540 residues (residues 4−543; 8279 atoms) for mAChE, 61 residues (906 atoms) for Fas2, 6 sodium counterions, and 35 796 solvent water molecules (including the crystallographic water molecules; 107 388 atoms): a total of 116 579 atoms.

The whole system was equilibrated with velocity reassignment every 1 ps (500 steps) at 50, 100, 200, and 298.15 K, for 20 ps (10 000 steps) each. Then it was equilibrated (without velocity reassignment) at 298.15 K for 1 ns (500 000 steps).

The equilibration and production parts of the simulation were performed on the Blue Horizon, an IBM Scalable POWERparallel (SP) supercomputer, at the San Diego Supercomputer Center. The production part was carried out over a period of 6 months (not continuous). The production jobs ran on 64−128 processors of the Blue Horizon, consuming about 75 processor-months of supercomputer time. Frames were collected at 1-ps intervals for the production length of 5 ns, giving 5×10^3 frames.

Proper Radii of the Passages. The extent of opening for every passage into the gorge was characterized using a single variable named the proper radius, as we introduced previously for the gorge in the apo-mAChE MD.[17,30] The proper radius was defined as the maximum radius of a spherical ligand that can go through the opening of interest from outside of the protein to reach the active site. This could be measured with an algorithm that finds the largest probe radius that generates the solvent-accessible surface with a continuous topology. Equivalently in practice, we detected whether the $O_{\epsilon 1}$ atom of Glu 202 contributes to a inflated solvent-accessible surface that connects to the outside of the protein. The probe was considered capable of entry into the active site when the residues outside and those inside are topologically continuous. With several trials for each snapshot, we could narrow down the proper radius to a desired resolution.

Three possible passages leading into the active site were located: the gorge, the side door, and the back door. While detecting for one potential opening, regions near the other two potential openings were blocked to avoid contamination. The gorge was blocked using a sphere centered at the average position of the atoms $C_{\delta 1}$ of Leu 76, C_β of Trp 286, and OH of Tyr 72, with a radius of 110 pm. The blocking sphere of the back door was centered at the center of the six-membered ring of Tyr 449, with a radius of 65 pm; that of the side door, at the C_β atom of Thr 75, with a radius of 91 pm. The proper radii for the side and back doors were only calculated if their values were larger than 140 pm at a resolution of 10 pm. A finer resolution (5 pm) was used for the gorge than for the doors, and no lower bound was imposed. Therefore, a discretized value of the gorge proper radius ρ means that the true value of the proper radius ρ^* satisfies $\rho - 2.5 \text{ pm} \le \rho^* < \rho + 2.5$ pm. For the doors, a value of proper radius ρ, when $\rho \ge 140$ pm, the true value of the proper radius ρ^* satisfies $\rho \le \rho^* < \rho + 10$ pm (Supporting Information).

Principal Component Analysis. The C_α coordinates of whole complex throughout the 5-ns trajectory (1803 degrees of freedom: 540 C_α atoms in mAChE, and 61 atoms in Fas2) were admitted into the principal component analysis (PCA):[31,32] The covariance matrix was constructed and then diagonalized to give the diagonal matrix of eigenvalues and the transformation matrix containing columns that were the eigenvectors. Using the transformation matrix, the projection time series along each one of the principal components was calculated. For each one of these principal components, the maximal and the minimal projections were transformed back to Cartesian coordinates.

Porcupine Plots. Porcupine plots[17] may be used to show the correlation between the movement of C_α atoms and any desired functionally important motion. In this case, the functionally important motions are the extent of opening of the gorge, the side door, and the back door.

The correlation coefficient between a proper radius $\rho(t)$ and the x degree of freedom for an C_α atom $x_i(t)$ was defined as

$$\frac{\langle (x_i(t) - \langle x_i \rangle_t)(\rho(t) - \langle \rho \rangle_t) \rangle_t}{\sqrt{\langle (x_i(t) - \langle x_i \rangle_t)^2 \rangle_t \langle (\rho(t) - \langle \rho \rangle_t)^2 \rangle_t}} \quad (1)$$

Similar expressions were obtained for $y_i(t)$ and $z_i(t)$ for the y and z coordinates. These three correlation coefficients made up a correlation vector for the C_α atom of each residue. The direction of the vector indicated where the residue was displaced when the proper radius became above average.

Results

The first part of the analysis compares mAChE in the present 5-ns simulation and our previous 10-ns simulation.[17] The differences in structure and dynamics of mAChE are investigated

(21) Bourne, Y.; Taylor, P.; Bougis, P. E.; Marchot, P. *J. Biol. Chem.* **1999**, *274*, 2963−2970.
(22) le Du, M.-H.; Housset, D.; Marchot, P.; Bougis, P. E.; Navaza, J.; Fontecilla-Camps, J. C. *Acta Crystallogr.* **1996**, *D52*, 87−92.
(23) Straatsma, T. P.; Philippopoulos, M.; McCammon, J. *Comput. Phys. Commun.* **2000**, *128*, 377−385.
(24) Cornell, W. D.; Cieplak, P.; Bayly, C. I.; Gould, I. R.; Merz, Jr., K. M.; Ferguson, D. M.; Spellmeyer, D. C.; Fox, T.; Caldwell, J. W.; Kollman, P. A. *J. Am. Chem. Soc.* **1995**, *117*, 5179−5197.
(25) Berendsen, H. J. C.; Grigera, J. R.; Straatsma, T. P. *J. Phys. Chem.* **1987**, *91*, 6269−6271.
(26) Berendsen, H. J. C.; Postma, J. P. M.; van Gunsteren, W. F.; Di Nola, A.; Haak, J. R. *J. Chem. Phys.* **1984**, *81*, 3684−3690.
(27) Darden, T.; York, D.; Pedersen, L. *J. Chem. Phys.* **1993**, *98*, 10089−10092.
(28) Ryckaert, J.-P.; Ciccotti, G.; Berendsen, H. J. C. *J. Comput. Phys.* **1977**, *23*, 327−341.
(29) van Gunsteren, W. F.; Berendsen, H. J. C. *Mol. Phys.* **1977**, *34*, 1311.
(30) Shen, T. Y.; Tai, K.; McCammon, J. A. *Phys. Rev. E* **2001**, *63*, 041902.
(31) García, A. E. *Phys. Rev. Lett.* **1992**, *68*, 2696−2699.
(32) Amadei, A.; Linssen, A. B.; Berendsen, H. J. *Proteins* **1993**, *17*, 412−425.

from RMSD plots, *B* factors, PCA, and average structures. The fluctuations in the width of the passages leading to the active site are examined, and porcupine plots are used to pick out the motions of residues involved in their opening. In the second part of the analysis, the relative motion of the two proteins is assessed, and the nature of the interface region in the Fas2−mAChE complex is inspected by looking at the dominant residue contacts, particularly those that change or diverge from the crystal structure with time.

Stability of the Trajectory and RMSD. The energy components, the temperature, and the volume were inspected and found to have reasonable stability throughout the 5-ns simulation (data not shown), ensuring that the system was at equilibrium. The RMSD of the protein structures from the crystal structure as a function of time for both heavy atoms and C_α atoms is in the Supporting Information. The RMSD for the heavy atoms in the complex fluctuated but stayed around 330 pm and, for the C_α atoms, around 280 pm. This is in contrast to the lower respective values in apo-mAChE of 170 and 120 pm. Thus, the simulated Fas2−mAChE complex appears to deviate more than apo-mAChE from the corresponding crystal structure. The mAChE part of the structure has even larger RMSD values through the 5 ns, but the fluctuation thereof is smaller than that of the whole complex.

Comparing the average structure from the production run with the crystal structure indicates the changes that occurred during the equilibration phase. These changes were mainly in the termini and the segments that were flexible in the production run. The active site residues had also changed in its conformation during equilibration; this change is shown below in detail.

Flexibility from *B* Factors. The isotropic temperature (*B*) factors provide a means of finding out which parts of the protein are behaving differently between apo-mAChE and Fas2−mAChE. *B* factors for our MD simulations were calculated from the mean square fluctuation (MSF)[33] (Supporting Information).

As in the apo-mAChE simulation, there is a wide variation in flexibility for different residues. To compare apo-mAChE and the complex, the ratio of the *B* factors calculated in the complex MD trajectory over those from the apo-mAChE MD for each residue is calculated (Supporting Information); this information may be marked onto the protein in Figure 2. The extent of positive deviation in complex ranges from blue (least) to red (most). Interestingly, deviations predominate around a number of residues and segments on the surface of the protein, namely, residues 46, 320, and 462 and the segments 258−264 (the distal small Ω loop) and 430−435. Overall, the *B* factors seen in the complex MD are larger and again support the overall trend that mAChE is more flexible in the complex than in the apo-form in our simulations.

Comparing the *B* factors for the Fas2 calculated from this simulation and the previous unbound Fas2 MD simulation,[34] we find that the flexibility in loops I (residues 4−16) and II (residues 23−38) that appeared in the unbound simulation has been suppressed compared to the flexibility in loop III (residues 42−51) and the two turn regions that encompass residues 16−20 and 54−57 near the Fas2 core.

Collective Motion from Principal Component Analysis. PCA is one means of displaying collective motion. The principal components with the largest eigenvalues represent the largest scale motions. The calculated eigenvalues decrease in magnitude quickly but smoothly: the eighth largest is less than 0.1 of the largest, and the 38th largest is less than 0.01 of the largest. The Cartesian coordinate structures for the maximal and minimal projections of the principal components with the two largest eigenvalues (1.58 and 0.87 nm^2) are shown in the Supporting Information.

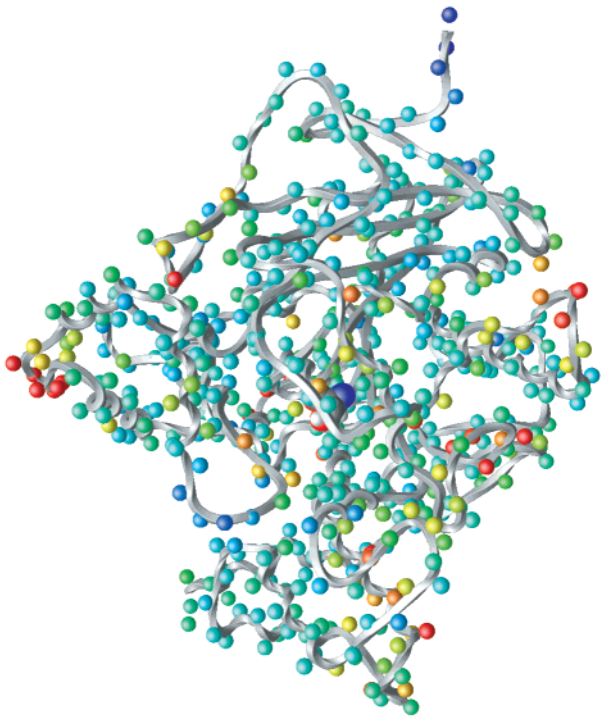

Figure 2. Ratio of *B* factor for each residue in mAChE, calculated as that from Fas2−mAChE MD over that from the apo-mAChE MD, colored on the mAChE structure; each sphere represents one residue. The ratio decreases from red to blue. The active site Ser 203 is shown in the space-filling representation. Generated using OpenDX (IBM, White Plains, New York) with Chemistry Modules.[44] See Supporting Information for another presentation of this comparison.

Comparing the Average Structures of mAChE. For both the apo-form and the complex simulations, we produced the average structure of mAChE by superimposing the enzyme conformations onto that in the crystal structure and taking the mean of the atom positions. The resulting two average structures are displayed in Figure 3. The distances between the C_α atoms and the absolute values of the ϕ and ψ angle differences for every residue in each average structure were calculated (Supporting Information). When comparing these average structures, we have to keep in mind that many differences in the distances and angles might be linked to the differences in crystal packing and in the resolutions of the starting crystal structures.

While the overall agreement between the two structures is close, there are many places where they differ in small ways, and in a few loops, the difference is quite substantial, such as residues 258−264 (the distal small Ω loop), 370−393, and 436−442, as well as the C-terminus. A greater variation is seen in the dihedral angles, but evidently many of these changes appear to cancel out and lead to little net movement in C_α position.

The active site arrangement was changed in the Fas2-bound complex, with critical implications for the function of mAChE.

(33) McCammon, J.; Harvey, S. *Dynamics of Proteins and Nucleic Acids*; Cambridge University Press: Cambridge, 1987.
(34) Baker, N. A.; Helms, V.; McCammon, J. A. *Proteins* **1999**, *36*, 447−453.

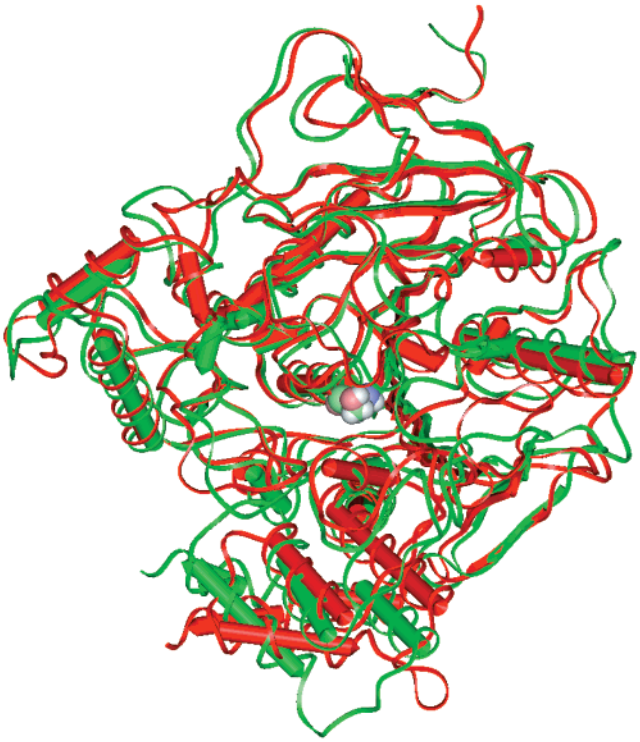

Figure 3. Comparing the average structures from the 10 ns apo-mAChE (red) and from the 5-ns Fas2−mAChE (green) trajectories. The backbones are displayed in the ribbon representation, with the α-helices and β-sheets shown. Residue Ser 203 from the average structure of the apo-mAChE trajectory is shown in the space-filling representation. Generated using Insight II. See Supporting Information for another presentation of this comparison.

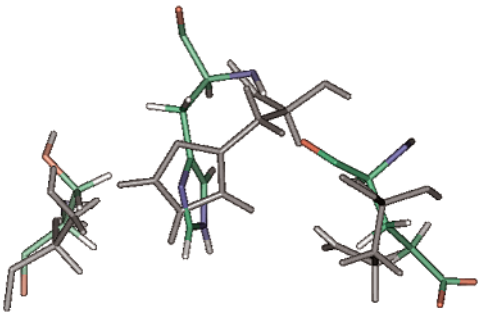

Figure 4. Catalytic triad of mAChE. The average structures from both simulations are shown, after all-atom superimposition of the mAChE molecule. Gray, the apo-mAChE MD; colored, from the Fas2−mAChE MD. From left to right, the residues are Ser 203, His 447, and Glu 334. Generated using Insight II.

The change was seen by comparing the average structures from the apo-form and the complex trajectories (Figure 4): In the apo-form average structure, the arrangement was conducive to proton transfer placing the imidazole ring of His 447 between the carboxyl group of Glu 334 and the hydroxyl group of Ser 203. Visual inspection of the complex trajectory and the average structure therefrom showed that, by many dihedral angle changes in the backbone and side chains, the His 447 imidazole ring moved to a conformation where it is almost orthogonal to the route of proton transfer. In addition, the side-chain carboxyl group of Glu 334 has moved away from the route. This disruptive change in conformation occurred in the 1-ns equilibration procedure before the 5-ns production run and persisted through the 5-ns production trajectory.

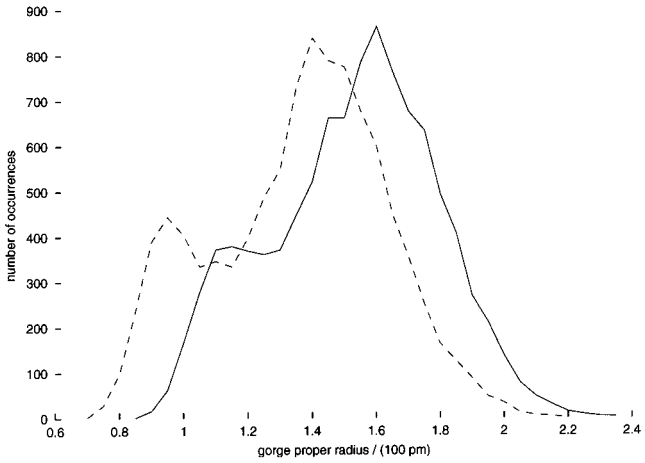

Figure 5. Distribution of the gorge proper radius. Solid line, that in the 10-ns apo-mAChE trajectory; dashed line, twice that in the 5-ns Fas2−mAChE trajectory (so normalized for ease of comparison with the 10-ns data).

Opening of the Passages. The one entrance into the active site that has been observed in all available crystal structures is the main active site gorge itself. The distribution for the gorge proper radius in the 5-ns Fas2−mAChE simulation is shown in Figure 5; the time series thereof is in the Supporting Information. As in the 10-ns apo-mAChE MD, we found two distinct local maxima in the probability distribution of the proper radius.[30] This affirms that there are indeed two states in mAChE gorge fluctuation: one narrower and one wider. In comparison, with Fas2 bound, the narrower state becomes more favored than in the apo-form simulation, and the distribution as a whole moves toward a smaller value for the gorge proper radius.

In addition, we produced the selective average structure for only the frames with an open gorge (proper radius greater than 127 pm) and that for only the frames with a closed gorge. The selective average structures for the open and closed versions do not appear to be significantly different. This is also true for the selective structures of the side door and those for the back door. (For these two, an opening is defined as having a proper radius greater than 140 pm.) If we focus on the gorge, the distance between the C_α atoms of Tyr 124 and Phe 338 that straddle the gorge in the selective average structure with an open gorge is 1.288 nm; the distance in the structure with a closed gorge is 1.281 nm; the difference is only 7 pm. For the apo-mAChE trajectory, the same distance measurement has 1.485 nm in the open gorge case and 1.440 nm in the closed case; the difference is 45 pm and is comparable to the difference in gorge radius between the two states seen in Figure 5.

A much larger and possibly functionally important difference was observed for the back and side doors. In the apo-form simulation, the back door was open to water molecules less than one-hundredth (0.01) of the frames and the side door was never observed to be open. However, in the complex, both side and back doors are observed to be open for a significant amount of simulation time. As shown in the Supporting Information, 917 out of the 5000 frames collected (0.18) have a back door opening event (proper radius larger than 140 pm); 664 out of the 5000 frames (0.13) have a side door opening event (defined likewise). There are 1158 frames (0.23) with either of the alternative passages open, and 423 frames (0.08) with both open.

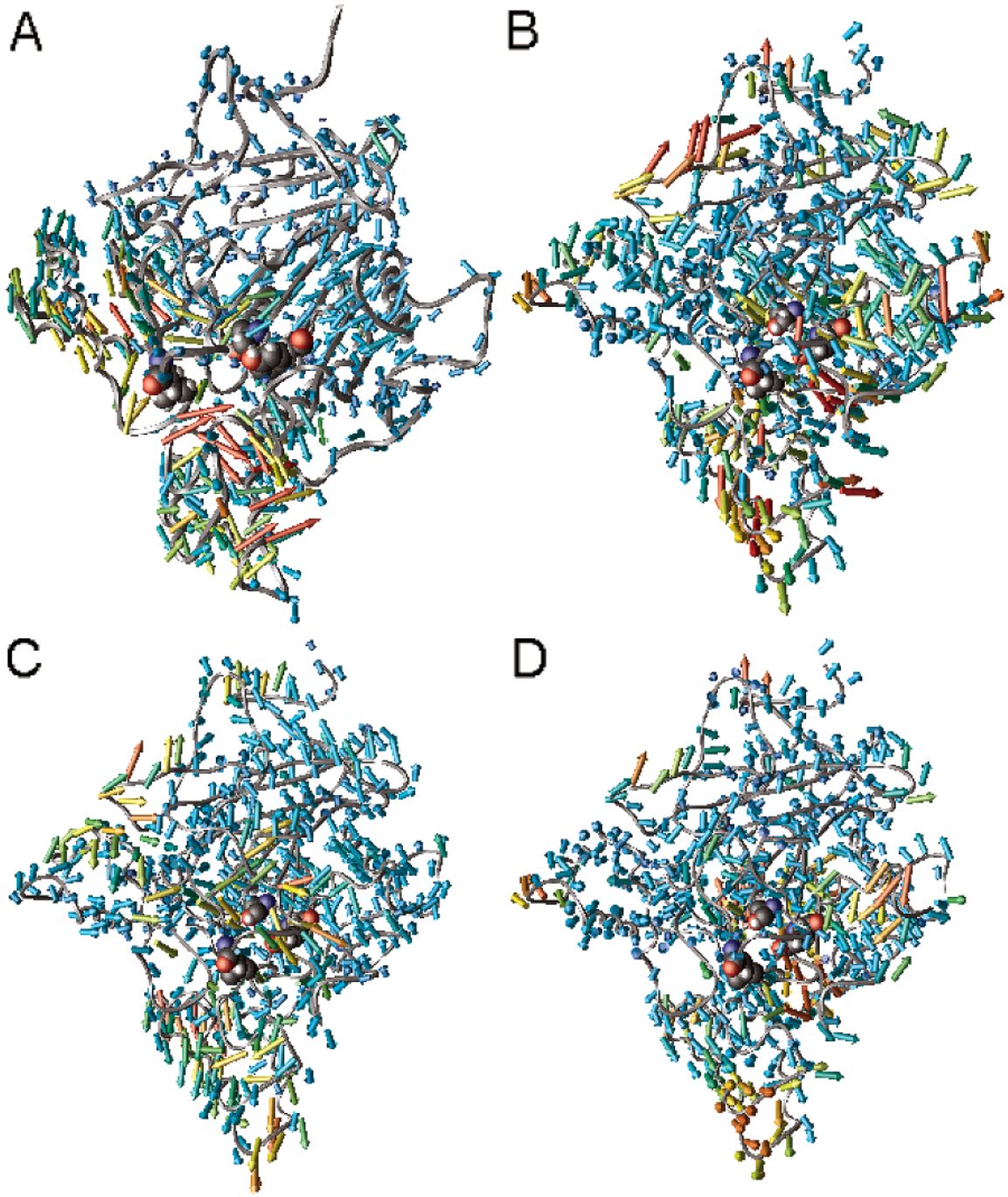

Figure 6. Porcupine plots. A, for the gorge in the apo-mAChE trajectory; B, for the gorge in the Fas2−mAChE trajectory. In these two, the same coloring scheme is used. C, for the side door in the Fas2−mAChE trajectory; D, for the back door in the Fas2−mAChE trajectory. In each, three residues are shown in the space-filling model: Ser 203 (marking the bottom of the gorge and the active site), top; Tyr 449 (marking the back door), right; Leu 76 (marking the side door), bottom left. Generated using OpenDX with Chemistry Modules.[44]

To probe the access to the active site by ligands or solvent molecules through the gorge when Fas2 is bound, we blocked the side and back doors and measured the largest opening in the gorge region with Fas2 in place. The gorge is open to a spherical probe of radius 140 pm in 233 frames (0.05), while in only 9 frames is the gorge open for a spherical probe of radius 160 pm.

Motions of Passages Using Porcupine Plots. Porcupine plots are an alternative means of displaying concerted protein motion. In the present work, they are used to extract out protein motion correlated with the radius of each passage found into the gorge. Three porcupine plots, for the gorge, the side door, and the back door, are shown in Figure 6. The coloring indicates the extent to which a residue's motion is correlated with the opening of the given passage, with red the most and blue the least.

Different parts of the protein are seen to be associated with each passage. Among the largest vectors in the side door porcupine plot is at residue 86, whose C_α atom is close to the side door region. Residues 445 and 446, in the back door region, have two of the largest vectors in the back door porcupine plot.

Movement and Contacts of Fas2. The first issue addressed here is the extent of Fas2 motion relative to mAChE. The trajectory of the center of geometry of Fas2 (defined as the average position of the C_α atoms) relative to that of mAChE

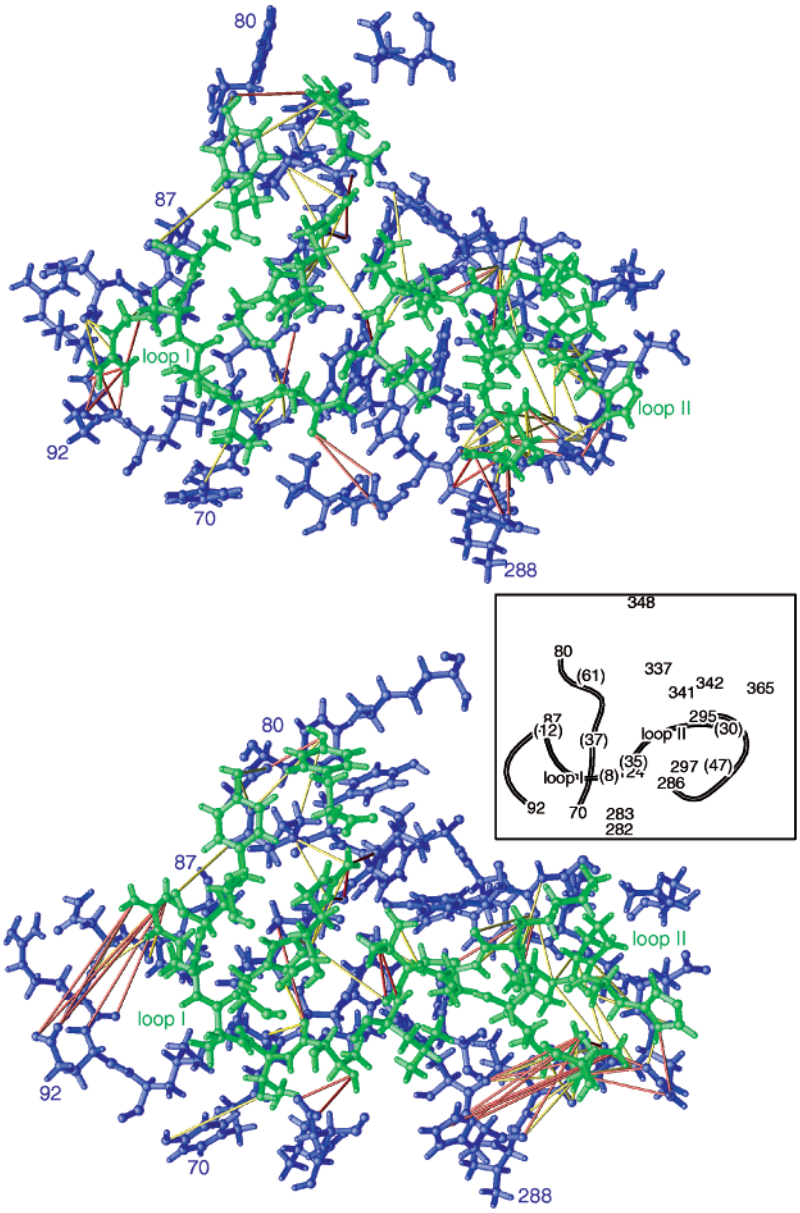

Figure 7. Interface contact pairs. Top, structure of the residues participating in contact at the start of the 5-ns production trajectory (at 0 ns; that is, right after the 1 ns equilibration); bottom, that at 5 ns. The residues shown are those participating in interfacial interactions more often than not during the 5 ns, both polar and nonpolar. Residues belonging to Fas2 are shown in green; those of mAChE, blue. The yellow bars represent polar interactions with only one maximum in the distance distribution (static); the red bars represent polar interactions with more than one maximum (dynamic). Generated using OpenDX with Chemistry Modules.[44] Inset, the backbone of the relevant segments in Fas2 (gray) and in mAChE (white), with key residues labeled (Fas2 in parentheses); generated using Molscript.[43]

was calculated. It was found that this Fas2 trajectory is contained within a sphere of radius 250 pm. Thus, it appears that the two proteins remain largely fixed with respect to each other for the duration of the simulation.

The second question is what residue contacts are made at the interface and whether any of these change. To pick out interesting contact pairs at the Fas2−mAChE complex interface, we record any distance between a heavy atom in Fas2 and another in mAChE that is shorter than 500 pm for more than half of the 5×10^3 frames in the 5-ns trajectory. There are 599 contact pairs between heavy atoms in the interface. Eighty-three of these are polar (between non-carbon heavy atoms) contact pairs; on the residue level, there are 39 interesting polar residue−residue contact pairs. For the 83 polar atom−atom pairs, we tallied the distributions of their distances through the 5-ns trajectory. If there is more than one maximum to a 50-pm resolution in a distribution, the residue can be considered more dynamic; otherwise, it is considered static, as the distance only fluctuates around one value. The details of these pairs are shown in Figure 7 and in the Supporting Information.

Discussion

Fas2 may influence the function of mAChE in a variety of complementary ways: Fas2 may sterically obstruct the entrance of the mAChE gorge, allosterically change the conformation of parts of the enzyme, affect the fluctuation behaviors of the openings dynamically, or affect the efficiency of the catalysis at the active site, among other things. Hence, our results will be discussed in light of these effects that may conceivably be adopted in the natural design of Fas2.

Steric Obstruction of the Gorge Entrance. As the eigenvalues from the PCA decrease rapidly in magnitude, the largest collective motions are represented in the few principal components with the largest eigenvalues. Looking at two of these components (Supporting Information), we do not see any collective movement that suggests Fas2 moving away significantly from the binding configuration where it sterically obstructs the gorge entrance. The Fas2 center of geometry movement relative to mAChE was also small; indeed, this motion can be contained by a sphere of radius 250 pm.

With Fas2 bound, the active site is rarely accessible through the gorge to allow entry of a spherical ligand with radius 160 pm (much smaller than the acetylcholine profile). Since it is nearly impossible for a ligand this size to move through the gorge, access to the active site is only likely through the alternative passages; in this simulation, we observed a large increase in their opening likelihood compared to the apo-mAChE trajectory.

Interactions at the Interface. The polar interface contact pairs are listed in the Supporting Information. The participating mAChE residues mostly fall into two groups: the Ω loop group (residues 69−96) and the residues near the peripheral site (roughly from Asp 283 to Ser 293, and Tyr 341). On the Fas2 side, the participating residues are mostly from loop I or II; only Asn 47 is from loop III, and Tyr 61 is at the C-terminus of Fas2. It is notable that nearly all Fas2 residues at this interface participate in polar interactions (Figure 7).

The contact regions of Fas2, namely, loops I and II, have higher or comparable flexibility compared to loop III in the previous unbound Fas2 simulation.[34] When bound to mAChE, they are surpassed in flexibility (measured by the *B* factors) by the noncontacting loop III.

Except for the few contacts made by the Fas2 core region, we do see most of the contacts reported in the crystal structure,[3] and when we do not see the exact interaction, usually a neighboring residue has a contact pair. In short, loops I and II of Fas2 have contacts with the mAChE Ω loop, while only loop II is in charge of interacting with the peripheral site. The flexibility of these contact loops is decreased relative to other parts of Fas2 upon binding.

Allostery: Changing the Conformation and Flexibility of mAChE. As we embark in comparing the apo-mAChE and the complex trajectories, there is a caveat we have to point out first: With nanosecond-scale simulations, the trajectories do not sample adequately all conformations available for a protein of the size of mAChE to explore. Some of the differences observed may be real and indicative of changes in protein functions under different circumstances; others may simply be trajectory-specific idiosyncracies that are imprudent to generalize.

Most residues in mAChE exhibited larger *B* factors in the Fas2−mAChE simulation than in the apo-mAChE one (Supporting Information). In particular, the distal small Ω loop from Pro 258 to Gly 264 had an extremely large increase in *B* factor as compared to that in the apo-mAChE simulation. Notably, this loop could not be resolved in the Fas2−mAChE complex crystal structures (1MAH and 1KU6)[3] because of its high flexibility, while in the tetrameric mAChE structure (1MAA),[21] where it participates in the crystalline tetramer interface and has stabilizing interactions, it was resolved in two of the monomers. The flexibility of this loop, as observed in the simulation, may be the reason for its low resolution in the complex structure.

Our previous apo-mAChE simulation[17] used the mAChE molecule from the Fas2−mAChE complex structure at 0.32-nm (3.2-Å) resolution (1MAA); the present Fas2−mAChE simulation used a Fas2−mAChE structure at 0.25-nm (2.5-Å) resolution, a resolution improvement that would be expected to generate lower *B* factors for the Fas2−mAChE simulation. Yet, we observed a higher flexibility in the complex trajectory than in the apo-mAChE trajectory.

By visual inspection, the most impressive differences between the mAChE structures from the apo-mAChE and Fas2−mAChE complex trajectories are in the positions and flexibilities of the distal small Ω loop from Pro 258 to Gly 264 (at the leftmost of Figure 3) and the remote segment around residue 380 (at the bottommost of the same figure). Despite being far from the Fas2 binding site, the distal small Ω loop seems to acquire a different average position and become more flexible (as seen in the *B* factors) upon Fas2 binding. This is in stark contrast with fluorescence spectroscopy results where the fluorophore attached at residue 262 of this distal loop indicated little alteration in flexibility.[35] To reconcile this discrepancy, we recall that the distal loop was built in artificially in the two MD simulations. Thus it may not be justified to compare the difference in flexibility in MD of this loop, considering its local lack of resolution in the crystal structure compounded with the ambiguity introduced by the artificial model-building process.

Dynamical Inhibition of Gorge Opening. Contrary to previous expectations,[3,21] the observed change in the fluctuation (as indicated by the *B* factors) and conformation of the Fas2-bound mAChE Ω loop are only moderate and not outstanding in view of other parts of the molecule. Evidence both from simulations and from fluorescence spectroscopy experiments[16] indicate that, though mAChE and *Candida rugosa* lipase are related in their α/β hydrolase fold, the former does not seem to have its open and closed states characterized by the well-defined hinge motion of the Ω loop as the latter.[36]

Considering that the two peaks in the probability distribution function of the gorge proper radius were separated by about 50 pm in the apo-mAChE trajectory,[30] it is not surprising that the difference between the Tyr 124−Phe 338 C_α distance is 45 pm. On the other hand, the smaller 7-pm difference in the complex trajectory manifests that the bottleneck region of the gorge is no longer coupled to the Tyr 124−Phe 338 distance upon Fas2 binding and implies significant change in the mechanism of the gorge opening behavior.

The binding of Fas2 indeed favors a narrower gorge size, as shown in Figure 5. Not only does the whole distribution shift toward a smaller value of the proper radius, but the narrower of the two distinct states becomes more likely to occur in the complexed trajectory. Comparing the porcupine plot for the gorge with that from the apo-mAChE MD,[17,37] we find that the

(35) Boyd, A. E.; Marnett, A. B.; Wong, L.; Taylor, P. *J. Biol. Chem.* **2000**, *275*, 22401−22408.
(36) Grochulski, P.; Li, Y.; Schrag, J. D.; Cygler, M. *Protein Sci.* **1994**, *3*, 82−91.
(37) Baker, N.; Tai, K.; Henchman, R.; Sept, D.; Elcock, A.; Holst, M.; McCammon, J. A. Mathematics and Molecular Neurobiology. In *Computational Methods for Macromolecules: Challenges and Applications: Proceedings of the 3rd International Workshop on Algorithms for Macromolecular Modelling*, New York, October 12−14, 2000; Schlick, T., Gan, H. H., Eds.; Lecture Notes in Computational Science and Engineering; Springer-Verlag: Berlin, in press.

concert of motions near the Fas2 interface seems to be repressed in the Fas2−mAChE trajectory. Such effect of dynamical inhibition[38] is impressive, though the mechanism by which Fas2 imposes this effect is still not clear to us.

Changes in the Alternative Passages to the Active Site. In contrast to the apo-mAChE trajectory where only 0.01 of all the frames collected gave an open back door,[17] we have an increase in the likelihood of opening to 0.18 when Fas2 is bound. In addition, the side door also has a 0.13 chance of being open in the complex trajectory (Supporting Information). In the porcupine plots, most concerted motions show up around the respective alternative passages (the side door and the back door). These increases in the number and likelihood of alternative openings, as previously suggested, may indeed be responsible for some of the residual, or even enhanced, substrate catalysis in Fas2-bound AChE.[3,11−13]

In a previous MD simulation of mAChE complexed with the active site ligand huperzine A,[39] opening of the side door is observed more frequently than in the apo-form simulation.[20] In another simulation, where the *T. californica* AChE dimer is complexed with the active site inhibitor tacrine,[19] side door opening is also observed. It is in this context that we report here the significant increase of side door opening events induced by an inhibitor that does not bind at the AChE active site. This implies that alternative passage opening events may be promoted by either active site or peripheral site binding.

Changes in the Conformation of the Active Site. Comparing the average structures (Figure 4) from the apo-mAChE and Fas2−mAChE trajectories, we notice dramatic differences in the mAChE catalytic triad: Upon Fas2 binding, the functional groups in Glu 334 and His 447 have moved out of the strategic positions conducive to proton transfer that are observed in the apo-mAChE MD and the crystal structure. Such movements are achieved through movements of the backbone and several dihedral angle changes in the side chains and do not appear to be trivial. Specifically, in the average structure from the Fas2−mAChE MD, the Glu 334 carboxylic group now points away from the neighboring His 447 in the complex MD, and the His 447 imidazole ring is now at an angle from its position in the apo-mAChE MD, out of alignment for proton transfer.

Crystallography of *T. californica* AChE complexed with the organophosphorus inhibitor VX showed a movement of the active site histidine.[40] Monoclonal antibodies that bind to the peripheral site have been reported to allosterically affect the orientation of Trp 86 near the active site.[41] In addition, kinetic data have suggested that Fas2 inhibits AChE by disrupting the conformation of the active site, thus slowing down the proton-transfer steps.[10] Our observation here is consistent with such a mechanism. However, as the Fas2 binding site does not neighbor the active site, the sequence of mechanical processes through which Fas2 exerts its influence is not immediately ostensible. Even though more rigorous procedures (such as the use of particle-mesh Ewald for the long-range electrostatics) were used here than the early MD work on *T. californica* AChE, where active site disruption was relieved by addition of absent counterions in the gorge,[42] the changes in the active site presently observed can only be considered suggestive at this stage.

Conclusions

In the Fas2−mAChE complex, Fas2 binds to the mAChE Ω loop and peripheral site with excellent surface complementarity using many polar and hydrophobic interactions from loops I and II.[3] Our 5-ns simulation of this complex shows that Fas2 binding dynamically disfavors the opening of the mAChE active site gorge but increases the likelihood for back door and side door opening, a feature that may contribute to the residual (and occasionally enhanced) catalytic activity of the Fas2-bound enzyme observed in solution. As in the apo-mAChE simulation, the fluctuating behavior of the mAChE gorge in the Fas2-bound complex continues to present complexity, though selective averaging suggests a change in the location of the bottleneck region. Fas2 binding also increases the flexibility of two surface segments remote to the binding site and, most impressively, disrupts the catalytic triad arrangement of the mAChE active site. In sum, we have observed steric, allosteric, and dynamic effects likely to represent the components of the mechanism through which Fas2 influences the function of mAChE.

Acknowledgment. We thank Dr. Tjerk P. Straatsma for providing and supporting the NWChem software, and Prof. Palmer W. Taylor, Dr. Zoran Radić, and Ms. Jianxin Shi for assistance and advice. Gratitude is expressed to Accelrys, San Diego, for providing us with the Insight II software, and to Dragon Farms, Toronto, for permission to use the photograph of *D. angusticeps* feeding in the table of contents. K.T. is a fellow of La Jolla Interfaces in Science training program, supported by Burroughs Wellcome Fund. This project was supported in part by Howard Hughes Medical Institute, W. M. Keck Foundation, San Diego Supercomputer Center, National Biomedical Computation Resource, National Science Foundation, and National Institutes of Health.

Supporting Information Available: Atom pairs with polar interactions at the Fas2−mAChE interface; stereograph of the Fas2−mAChE crystal structure; time series for the openings; RMSD and *B* factor data; extremal projections from PCA; comparison of the average structures from the trajectories (PDF). This material is available free of charge via the Internet at http://pubs.acs.org. See any current masthead page for ordering information and Web access instructions.

JA017310H

(38) Zhou, H.-X.; Wlodek, S. T.; McCammon, J. A. *Proc. Natl. Acad. Sci. U.S.A.* **1998**, *95*, 9280−9283.
(39) Tara, S.; Helms, V.; Straatsma, T. P.; McCammon, J. A. *Biopolymers* **1999**, *50*, 347−359.
(40) Millard, C. B.; Koellner, G.; Ordentlich, A.; Shafferman, A.; Silman, I.; Sussman, J. L. *J. Am. Chem. Soc.* **1999**, *121*, 9883−9884.
(41) Saxena, A.; Hur, R.; Doctor, B. P. *Biochemistry* **1998**, *37*, 145−154.
(42) Axelsen, P. H.; Harel, M.; Silman, I.; Sussman, J. L. *Protein Sci.* **1994**, *3*, 188−197.
(43) Kraulis, P. J. *J. Appl. Crystallogr.* **1991**, *24*, 946−950.
(44) Gillilan, R. E.; Wood, F. *Comput. Graphics* **1995**, *29*, 55−58.